Structural Investigations of xV$_2$O$_5$-(100-x)B$_2$O$_3$ Glass Matrix by Spectroscopic Techniques

RAJESH KUMAR SHARMA[*] and V. ILAMATHI

Department of Chemistry, Kanchi Mamunivar Centre for Post Graduate Studies, Pondicherry-605008, India

*Corresponding author: E-mail: rksepr@gmail.com

Preparation of glasses of xV$_2$O$_5$-(100-x) B$_2$O$_3$ ($21 \leq x \leq 41$) system for x = 21, 31, 41 mol % have been performed using sol-gel process and studied by employing XRD, FT-IR, EPR and UV-visible techniques. The glassy phase was established by powder XRD patterns. Fourier transform infrared red studies of the amorphous samples revealed the appearance of triangular [BO$_{3/2}$] and tetrahedral [BO$_{4/2}$] and V = O units. X-band powder EPR studies exhibit partially resolved isotropic lines at 300 K and well resolved hyperfine structure having a 16 line features (8 parallel lines and 8 perpendicular lines) at 77 K. The assignment of EPR parameters, g$_{xx}$ = g$_{yy}$ = g$_\perp$ > g$_{zz}$ = g$_\parallel$ and A$_{zz}$ = A$_\parallel$ > A$_{xx}$ = A$_{yy}$ = A$_\perp$ is consistent with ground state ^{2}B$_2$ which confirms that the tetravalent vanadium (3d^1) exists in the glass matrix as vanadyl ion in tetragonally distorted compressed octahedral symmetry having C$_{4v}$ symmetry. UV-visible absorption spectra of glasses exhibit characteristic two ligand field *d-d* bands in the tetragonal fields of VO^{2+} ions. Using EPR parameters and UV-visible data, various molecular orbital bonding parameters were ascertained.

Keywords: Vanadium pentoxide, Boric acid, Glass matrix, Bonding coefficients.

INTRODUCTION

During recent times transition metal oxide glasses prepared by sol-gel method have provided several advantages like studying properties of glasses at room temperature. Borate glasses of oxides of vanadium, copper and iron have been studied extensively because of their numerous uses as optical, magnetic and electronic materials [1]. Boron trioxide has been considered to be the best glass forming non-metallic oxides which revealed the formation of boroxol rings composing of two dimensional three-coordinate BO$_3$ groups [2] in glass network of boron trioxide. It was reported that in the presence of V$_2$O$_5$ as glass modifier, transformation of planar BO$_3$ groups into tetrahedral BO$_4$ groups takes place with the making of diborate [B$_2$O$_5$]$^{4-}$, triborate [B$_3$O$_6$]$^{3-}$ and polyborate [(BO$_2$)$^-$]$_n$ [3]. Vanadium pentoxide-boron trioxide glass systems display various structural aspects of properties because of the existence of multiple oxidation states of vanadium. The nature of 3d electron in vanadyl glass matrices was interpreted by a significantly stable V = O bond and because of it most of the vanadyl glasses are found to have five-coordinated square pyramidal geometry with C$_{4v}$ symmetry [4]. The existence of tertavalent vanadium

(3d^1) was studied as a paramagnetic vanadyl ion in the glass matrices containing V$_2$O$_5$ [5]. Tetravalent vanadium is stabilized by dπ-pπ (V = O) as the most stable oxocation, VO^{2+}. EPR studies have given significant information concerning the geometry around VO^{2+} due to change in the ligand field [6]. Glasses containing vanadyl ions display excellent semiconducting property because the excited small polarons [7,8] hop from a V^{4+} sites (3d^1) to a V^{5+} site. EPR results in combination with optical data are utilized to investigate the symmetry and different types of bonding in vanadyl glasses. On account of relatively longer spin lattice relaxation time and high I = 7/2, electron paramagnetic resonance studies of VO^{2+} ion (3d^1) are easily done even at room temperature apart from studying at lower temperature. X-band EPR spectral analysis of glasses containing VO^{2+} ion in tetragonally compressed octahedral entity [9,10] gives the following characteristic parameters, g$_{xx}$ = g$_{yy}$ = g$_\perp$ > g$_{zz}$ = g$_\parallel$ and A$_{zz}$ = A$_\parallel$ > A$_{xx}$ = A$_{yy}$ = A$_\perp$. The spin Hamiltonian parameters obtained in this paper shows similar results.

Electron paramagnetic resonance lines and structure of oxide glasses [11,12] containing vanadyl ions were investigated extensively. The concept of polar on hopping is used to study the conductivity in P$_2$O$_5$-V$_2$O$_5$-Na$_2$O [13], V$_2$O$_5$-Sb-TeO$_2$ [14]

and V_2O_5-NiO-TeO_2 [15] amorphous systems. The structure of glasses of V_2O_5 doped ZnO [16], vanadium pentoxide and fluoro germinate [17] and vanadate lithium borate system [18] has been investigated by electron paramagnetic resonance studies. Semiconducting properties of glass matrix of barium vanadate glass doped with iron oxides [19] have been reported. EPR and UV-visible investigations of vanadyl ions, VO^{2+} in glass matrices of VO^{2+}: Li_2O-K_2O-Bi_2O_3-B_2O_3 [20], vanadyl doped Bi_2O_3-B_2O_3-Li_2O [21], VO^{2+} ions in zinc lead borate glasses [22] have been communicated. Infrared and EPR studies of glass system consisting of lithium borate and VO^{2+} ions have been elucidated by Cozar *et al.* [23].

The X-band powder EPR lineshapes of glasses exhibit significant changes in spin-Hamiltonian parameters and hyperfine coupling when the temperature is lowered from 300 to 77 K. The partially resolved X-band EPR of VO^{2+} at 300 K changes into a fully resolved hyperfine structure at 77 K due to the coupling of ^{51}V nucleus having I = 7/2 with the unpaired electron of tetravalent vanadium. Thermal hopping rate of small polaron, $V^{4+}(3d^1)$ influence modulation of EPR lineshapes [24]. The calculated spin-Hamiltonian parameters from X-band powder electron paramagnetic resonance line shapes at 300 K and 77 K confirm that bonding around V^{4+} in glass samples is different. The nature of bonding in glasses is explained by bonding parameters which is obtained by correlating liquid nitrogen EPR results and UV-visible data. In present work, the results are presented regarding the investigation of the structure of glass matrix obtained with the variation in the glass composition by means of powder XRD, FT-IR, variable temperature X-band powder EPR and UV-visible spectroscopic techniques.

EXPERIMENTAL

Sol-gel procedure was employed to prepare three glass samples A1, A2 and A3 of compositions xV_2O_5-(100-x) B_2O_3 (21 ≤ x ≤ 41) from reagent grade chemicals. Batches for each glass consisting of calculated quantities of vanadium pentoxide [V_2O_5], orthoboric acid [H_3BO_3] and citric acid were prepared by means of melting in silica crucibles in the temperature range 963-973 K. The preparation of glasses is achieved by compressing molten liquid between two folds of ice cold aluminum plates through air quenching. Synthesized samples are grounded to obtain a very fine powder for investigating various properties. Amorphous phase was determined with the studies of powder XRD patterns recorded on Philips X' pert with CuK_α radiation. The infrared spectra of glassy samples were studied by Shimadzu spectrometer with the help of potassium bromide pellet process in the range 4000-400 cm^{-1}. Powder X-band EPR spectral studies were performed by JES-FA200 spectrometer having a 100 kHz field modulation at 300 and 77 K. The room temperature UV-visible absorption spectra were obtained by JASCO UV-visible spectrophotometer having wavelength range of 1000-400 nm.

RESULTS AND DISCUSSION

The XRD measurement was utilized to characterize glassy phase in the prepared samples. Room temperature powder XRD patterns of glass matrix are represented in Fig. 1. The XRD patterns of the samples show characteristic amorphous

phase due to the presence of a broad and diffuse peak at 30° without sharp and narrow peak at higher diffraction angle. Room temperature FT-IR spectra of xV_2O_5-(100-x) B_2O_3 glass samples are presented in Fig. 2. Infrared spectral studies are utilized to find the presence of structural groups in the glass matrix. A sharp band corresponding to symmetric bending vibration of O-B-O of [$BO_{3/2}$] unit [25] is found in 546-545 cm^{-1} region and intensity of this peak increases from A1 to A3. The bending mode of B-O-B group [26] is represented by a less intense band at ~ 645-644 cm^{-1} in the glass samples A1 to A3. The stretching vibration of the V-O-V unit [27] in all glass matrixes is shown by a sharp and broad band at ~ 781 cm^{-1} due to high concentration of V_2O_5. A weak band having B-O stretching vibrations [28] characteristic of BO_4 units in diborate groups and a stretching vibration of V=O unit [29] are observed at ~ 884-882 cm^{-1}.
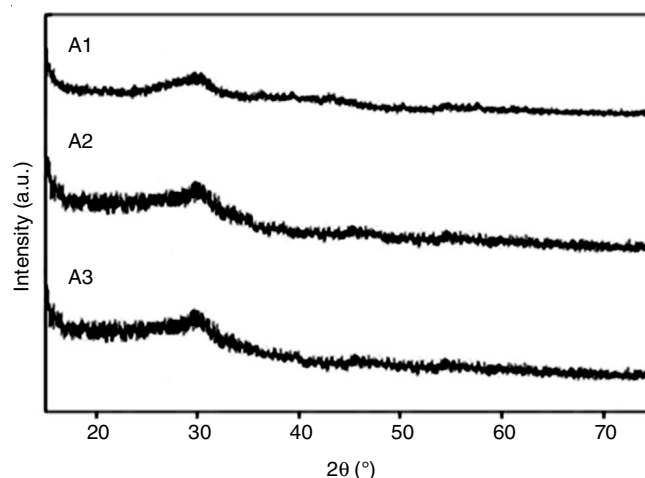

Fig. 1. PXRD pattern of xV_2O_5-(100-x) B_2O_3 (21 ≤ x ≤ 41) glasses
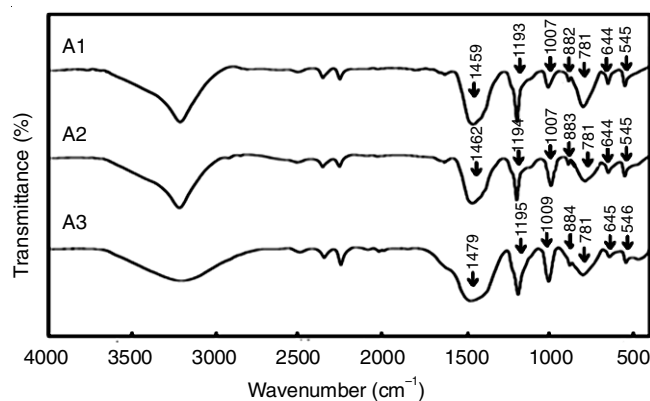

Fig. 2. Infrared spectra of V_2O_5-B_2O_3 glass matrix

The strong band at about 1009-1007 cm^{-1} region is characterized by the asymmetric vibrational mode of isolated non-bridging V=O bond [30] of VO_5 arrangement in glass samples A1-A3. The intensity of asymmetrical stretching vibration of isolated non-bridging V=O bond is found to enhance with the increase in the concentration of V_2O_5. An asymmetrical vibrational mode of B-O bond in pyro and orthoborate groups in [$BO_{3/2}$] units [28] is confirmed by an intense band in the range 1195-1193 cm^{-1}. A broad and intense band in 1479-1459 cm^{-1} region is on account of antisymmetric vibrational mode of

B-O-B units [26] in the glasses which arise due to linkage between planar [BO$_{3/2}$] and tetrahedral [BO$_{4/2}$] groups. The X-band powder EPR lines of glass matrix measured at 300 K and liquid nitrogen temperature are depicted in Fig. 3. Electron paramagnetic resonance line shapes show partially resolved isotropic hyperfine structures exhibiting perpendicular feature with very poor parallel feature at 300 K. This partially resolved hyperfine line is attributed to the rapidly activated hopping of a small polaron from a V^{4+} (3d^1) to V^{5+} (3d^0) and the anisotropic hyperfine features gets smeared out to give isotropic lineshapes at 300 K. When the temperature is reduced from 300 to 77 K, EPR spectra displayed significant changes in their hyperfine structural features. The glass samples exhibit a fully resolved anisotropic hyperfine feature consisting of 8 parallel and 8 perpendicular lines due to slow hopping rate of polaron at 77 K. The fully resolved EPR hyperfine structure is characteristic feature of VO^{2+}, arising because of interaction of unpaired 3d^1 electron of VO^{2+} ion with the nuclear spin quantum number of vanadium nucleus in an axially symmetric ligand field. The EPR spectral studies indicate that V^{4+} exist as VO^{2+} in C$_{4V}$ symmetry with 3d_{xy} as ground state [31]. The EPR lineshapes of vanadyl ion are elucidated by the following spin-Hamiltonian operator [32].
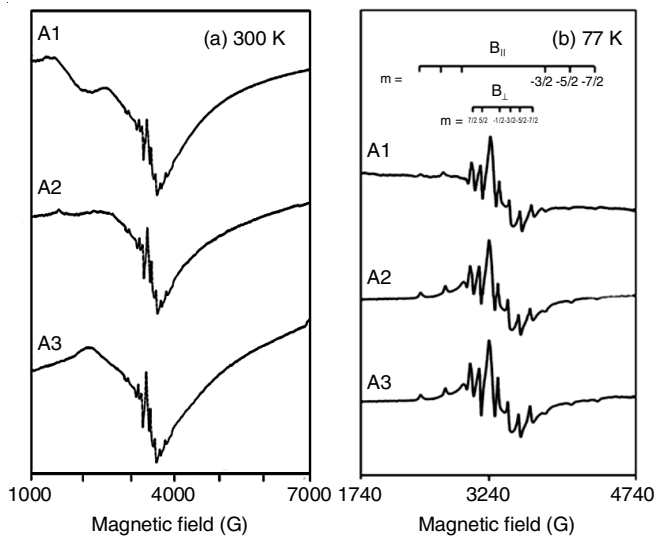

Fig. 3. X-band powder EPR spectra of xV₂O₅-(100-x)B₂O₃ (21 ≤ x ≤ 41) glass matrix at (a) 300 K and (b) 77 K

$$H = \beta_e\, g_{\parallel}\, H_z\, S_z + \beta_e\, g_{\perp}\, (H_x\, S_x + H_y\, S_y) + A_{\parallel}\, I_z\, S_z + A_{\perp}\, (S_x\, I_x + S_y\, I_y) \tag{1}$$

From partially resolved EPR spectra in A1-A3 at 300 K, the calculated isotropic g-value is found to be 1.97. The anisotropic spin-Hamiltonian parameters evaluated from observed X-band EPR lines at 77 K are presented in Table-1. Negative g-shift is shown by the samples at 300 and 77 K because of positive sign of λ. The spin-Hamiltonian parameters A$_{\parallel}$, A$_{\perp}$, g$_{\parallel}$ and g$_{\perp}$ obtained from EPR spectra in the given range of temperature are related to the local symmetry of the crystal field. The EPR parameters show similarity with the reported values of vanadyl glasses [33,34]. The EPR parameters, g$_{zz}$ = g$_{\parallel}$ < g$_{xx}$ = g$_{yy}$ = g$_{\perp}$ < g$_e$ and A$_{zz}$ = A$_{\parallel}$ > A$_{xx}$ = A$_{yy}$ = A$_{\perp}$ [35] are characteristic of vanadyl ion in tetragonally distorted octahedral environment. Different g- and A-values may be assigned

TABLE-1
EPR POWDER PARAMETERS OF xV₂O₅-(100-x) B₂O₃ (21 ≤ x ≤ 41) GLASS MATRIX AT LNT

Sample No.	g$_{\parallel}$	g$_{\perp}$	A$_{\parallel}$ (0.0001/cm)	A$_{\perp}$ (0.0001/cm)
A1	1.932	1.973	166	69
A2	1.934	1.975	170	70
A3	1.934	1.975	170	70

to the overall ligand field effect in the glass network caused by the change in temperature at 300 and 77 K. The similar g-values at different concentrations in the samples A1-A3 at 300 K indicate identical symmetry and environment around paramagnetic site. The changes in EPR parameters, g- and A- at 77 K at variable concentrations in the samples A1-A3 show that the distorted octahedral geometry is dissimilar in terms of nature of bonding centered at VO^{2+} ion. It is also confirmed that VO^{2+} ion is a paramagnetic site where V^{4+} exists in a tetragonally compressed octahedral symmetry. The EPR results are in good agreement with FT-IR studies in terms of geometry of VO^{2+} ion.

UV-visible absorption spectra of xV₂O₅-(100-x) B₂O₃ glass samples measured at 300 K in the region of wavelength of 400-1000 nm are depicted in Fig. 4. In a regular octahedral symmetry of VO^{2+} ions, a single d-d band with respect to the transition, ^{2}T$_{2g}$ → ^{2}E$_g$ is anticipated. EPR studies at 300 K and 77 K confirm that there is tetragonal distortion in octahedral coordination entity. In a tetragonal symmetry (C$_{4v}$), the ground state of VO^{2+} (3d^1) ion is 3d_{xy}. For VO^{2+} ions, three expected d-d bands are ^{2}B$_2$ → ^{2}E (3d$_{xy}$→3d$_{xz}$, 3d$_{yz}$), ^{2}B$_2$ → ^{2}B$_1$ (3d$_{xy}$→ 3d$_{x^2-y^2}$) and ^{2}B$_2$ → ^{2}A$_1$ (3d$_{xy}$→3d$_{z^2}$) the transitions [36,37] in tetragonal field. The two broad and intense d-d transitions, ^{2}B$_2$ → ^{2}E and ^{2}B$_2$ → ^{2}B$_1$ occur at ~ 840 - 860 nm and at ~ 680 - 690 nm respectively. The transition ^{2}B$_2$ → ^{2}B$_1$ is a measure of 10 Dq. The presence of two d-d transitions, ^{2}B$_2$ → ^{2}E and ^{2}B$_2$ → ^{2}B$_1$ are characteristic to VO^{2+} ions in octahedral symmetry having tetragonal compression.
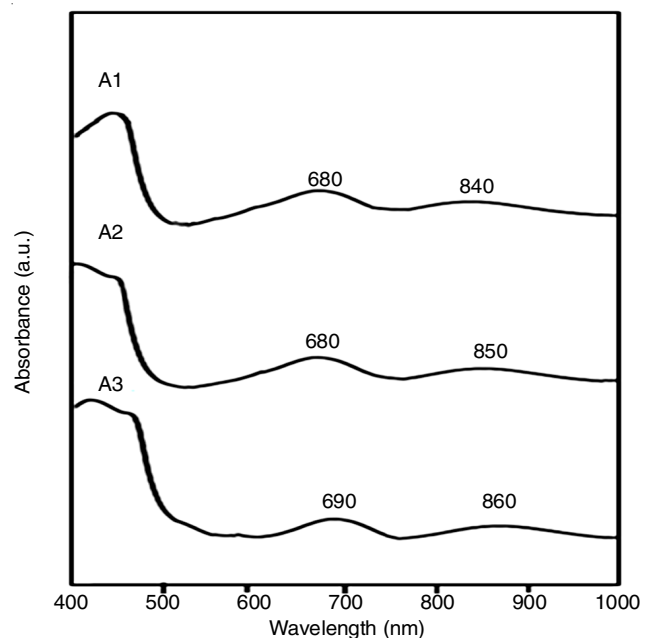

Fig. 4. UV-visible absorption spectra of xV₂O₅-(100-x) B₂O₃ (21 ≤ x ≤ 41) glass matrix

The UV-visible spectral results are in conformity with EPR studies in terms of local geometry and site symmetry. The data obtained from EPR studies at 77 K and UV-visible results are correlated to the M O bonding parameters according to the formulae [38].

$$g_{\parallel} = g_e \left[1 - 4\lambda\, \beta_1^2\beta_2^2/\Delta E_1\, (^2B_{2g}\rightarrow{}^2B_{1g})\right] \tag{2}$$

$$g_{\perp} = g_e \left[1 - 2\lambda\, \beta_2^2\gamma^2/\Delta E_2\, (^2B_{2g}\rightarrow{}^2E_g)\right] \tag{3}$$

where, g_e and $\lambda = 170$ cm^{-1} [23] are free electron g-value and spin-orbit coupling constant of V^{4+} ion respectively. In eqns. 2 and 3, the terms β_1^2, β_2^2 and γ^2 explain in-plane σ bonding, in-plane π bonding and out-of-plane π bonding, respectively [39]. The calculated g- and A-values, $g_{\parallel}$, $g_{\perp}$ and $A_{\parallel}$, $A_{\perp}$ are correlated to the M O parameters by the eqns. 4 and 5.

$$A_{\parallel} = p \left[- k - 4/7\, \beta_2^2 + 3/7\, (g_{\perp}-g_e) + (g_{\parallel}-g_e)\right] \tag{4}$$

$$A_{\perp} = p \left[- k + 2/7\, \beta_2^2 + 11/14\, (g_{\perp}-g_e)\right] \tag{5}$$

By combining eqns. 4 and 5, an expression of β_2^2 in terms of EPR data, $A_{\parallel}$, $A_{\perp}$, $g_{\parallel}$ and $g_{\perp}$ is obtained.

$$\beta_2^2 = (-7/6) \left[(A_{\parallel}-A_{\perp})/p + (g_e-g_{\parallel}) - (5/14)(g_e-g_{\perp})\right] \tag{6}$$

Eqns. 2 and 3 are used to calculate β_1^2 and γ^2. Using p for V^{4+} ions as 0.0128 cm^{-1}, β_2^2 the k are calculated with the help of eqns. 4 or 5. These bonding parameters are presented in Table-2. k describes density of unpaired electron at the V^{4+} ions and mixing of 4s orbital into 3d$_{xy}$ in tetragonal field. β_2^2 clearly shows poor in plane π bonding in V=O. γ^2 is lower than β_1^2 confirming that out of plane π bonding is moderately ionic and in plane σ bonding is more ionic.

TABLE-2
MOLECULAR BONDING COEFFICIENTS AND DEGREE OF
COVALENCE OF VO^{2+} IN xV$_2$O$_5$-(100-x) B$_2$O$_3$ ($1 \le x \le 41$)
GLASS MATRIX SYSTEM AT LNT

Sample No.	β_2^2	β_1^2	γ^2	k
A1	0.81	0.937	0.633	0.750
A2	0.84	0.878	0.561	0.768
A3	0.84	0.865	0.555	0.768

Conclusion

XRD analysis confirms amorphous nature in the samples. FT-IR analysis reveal the presence of prominent groups like triangular [BO$_{3/2}$] and tetrahedral [BO$_{4/2}$] and V=O units in the network of glass matrix. EPR lineshapes show partially resolved isotropic hyperfine feature exhibiting more perpendicular and less parallel feature at 300 K. The g- and A-values from powder X-band EPR lineshapes at 77 K show that tetravalent vanadium exists as vanadyl ion in tetragonally compressed octahedral environment having C$_{4v}$ symmetry. UV-visible studies indicate that two *d-d* bands assigned to the transitions $^2B_2\rightarrow{}^2E$ (3d$_{xy}\rightarrow$3d$_{xz}$, 3d$_{yz}$) and $^2B_2\rightarrow{}^2B_1$ (3d$_{xy}\rightarrow$3d$_{x^2-y^2}$) are characteristic of vanadyl ions in tetragonal field. The molecular bonding coefficients obtained by combining EPR results at 77 K and UV-visible data of VO^{2+} ions have revealed that in plane π bonding character in V=O is poor. From the numerical values of γ^2 and β_1^2, it is found that out of plane π bonding is moderately ionic in nature and in plane σ bonding is more ionic.

CONFLICT OF INTEREST

The authors declare that there is no conflict of interests regarding the publication of this article.

REFERENCES

1. R.A. Montani, M. Levy and J.L. Souquest, *J. Non-Cryst.* Solids, **149**, 249 (1992);
https://doi.org/10.1016/0022-3093(92)90073-S.
2. R.A. Smith, *J. Non-Cryst Solids*, **84**, 421 (1986);
https://doi.org/10.1016/0022-3093(86)90805-7.
3. L. Baia, R. Steefan, J. Popp, S. Simon and W. Kiefer, *J. Non-Cryst. Solids*, **324**, 109 (2003);
https://doi.org/10.1016/S0022-3093(03)00227-8.
4. R.V.S.S.N. Ravikumar, V.R. Reddy, A.V. Chandrasekar, B.J. Reddy, Y.P. Reddy and P.S. Rao, *J. Alloys Compds*, **337**, 272 (2002);
https://doi.org/10.1016/S0925-8388(01)01963-6.
5. K.V. Narasimhulu and J.L. Rao, *Spectrochim. Acta A Mol. Biomol. Spectrosc.*, **53**, 2605 (1997);
https://doi.org/10.1016/S1386-1425(97)00196-0.
6. G. Hochstrasser, *Phys. Chem. Glasses*, **7**, 178 (1966).
7. G.N. Greaves, *J. Non-Cryst. Solids,* **11**, 427 (1973);
https://doi.org/10.1016/0022-3093(73)90089-6.
8. F.R. Landsberger and P.J. Bray, *J. Chem. Phys.*, **53**, 2757 (1970);
https://doi.org/10.1063/1.1674400.
9. R.R. Kumar, A.S. Rao and B.C. Venkata Reddy, *Opt. Mater.*, **4**, 723 (1995);
https://doi.org/10.1016/0925-3467(95)00021-6.
10. R.P. Sreekanth Chakradhar, G. Sivaramaiah, J.L. Rao and N.O. Gopal, *Modern Phys. Lett. B*, **19**, 643 (2005);
https://doi.org/10.1142/S021798490500861X.
11. D. Kivelson and S.K. Lee, *J. Chem. Phys.*, **41**, 1896 (1964);
https://doi.org/10.1063/1.1726180.
12. H.G. Hecht and T.S. Johnston, *J. Chem. Phys.*, **46**, 23 (1967);
https://doi.org/10.1063/1.1840378.
13. M.C. Ungureanu, M. Levy and J. Souquet, *J. Ceramics Silikaty*, **44**, 81 (2000).
14. H. Mori, H. Matsuno and H. Sakata, *J. Non-Cryst. Solids.* **276**, 78 (2000);
https://doi.org/10.1016/S0022-3093(00)00280-5.
15. K. Sega, H. Kasai and H. Sakata, *Mater. Chem. Phys.*, **53**, 28 (1998);
https://doi.org/10.1016/S0254-0584(97)02052-X.
16. S. Karamat, R.S. Rawat, P. Lee, T.L. Tan, R.V. Ramanujan and W. Zhou, *Appl. Surf. Sci.*, **256**, 2309 (2010);
https://doi.org/10.1016/j.apsusc.2009.09.039.
17. L.D. Bogomaolva, N.A. Krasilnikova, V.L. Bogdanov, V.D. Khalilev and V.V. Mitrofanov, *J. Non-Cryst. Solids*, **188**, 130 (1995);
https://doi.org/10.1016/0022-3093(95)00098-4.
18. O. Cozar, I. Ardelean, V. Simon, G. Ilonca, C. Crocium and C. Cefan, *J. Alloys. Compd.*, **326**, 124 (2001);
https://doi.org/10.1016/S0925-8388(01)01247-6.
19. Y.M. Moustafa, I.A. Gohar, A.A. Megahed and E.L. Mansour, *Phys. Chem. Glasses*, **38**, 92 (1997).
20. M. Subhadra and P. Kistaiah, *J. Alloys. Compd.*, **505**, 634 (2010);
https://doi.org/10.1016/j.jallcom.2010.06.097.
21. A. Agarwal, V.P. Seth, P.S. Gahlot, S. Khasa, M. Arora and S.K. Gupta, *J. Alloys Compd.*, **377**, 225 (2004);
https://doi.org/10.1016/j.jallcom.2004.01.057.
22. P.G. Prakash and J.L. Rao, *Spectrochim. Acta A Mol. Biomol. Spectrosc.*, **61**, 2595 (2005);
https://doi.org/10.1016/j.saa.2004.09.025.
23. O. Cozar, I. Ardelean, I. Bratu, V. Simon, C. Cracium, L. David and C. Cefan, *J. Mol. Struct.*, **563**, 421 (2001);
https://doi.org/10.1016/S0022-2860(01)00442-2.
24. P. Raghunatha and B.B. Das, *Chem. Phys. Lett.*, **160**, 627 (1989);
https://doi.org/10.1016/0009-2614(89)80076-4.
25. E.I. Kamitsos, M.A. Karakassides and G.D. Chryssikos, *Phys. Chem. Glasses*, **30**, 229 (1989).
26. Y.Y. Kim, K.H. Kim and J.S. Choi, *J. Phys. Chem. Glasses*, **50**, 903 (1989).

27. T.R. Gilson, O.F. Bizri and N. Cheethham, *J. Chem. Soc. Dalton Trans*., 291 (1973);
    https://doi.org/10.1039/DT9730000291.

28. E.I. Kamitsos, M.A. Karakassides and G.D. Chryssikos, *J. Phys. Chem*., **91**, 1073 (1987);
    https://doi.org/10.1021/j100289a014.

29. F.A. Cotton, G. Wilkinson, C.A. Murillo and M. Bochmann, Advanced Inorganic Chemistry, Wiley: New Delhi, India, edn 6, pp. 723-725 (2008).

30. V.A. Kolesova and F.K. Stek, *J. Glass Technol.*, **12**, 1 (1986).

31. F. Tian, X. Zhang and L. Pan, *J. Non-Cryst. Solids*, **105**, 263(1988);
    https://doi.org/10.1016/0022-3093(88)90316-X.

32. O. Cozar, I. Ardelean, V. Simon, L. David, V. Mih and N. Vedean, *Appl. Magn. Reson*., **16**, 529 (1999);
    https://doi.org/10.1007/BF03161948.

33. H. Toyuki and S. Akagi, *Phys. Chem. Glasses*, **13**, 15 (1972).

34. J.R. Pilbrow, Transition Ion Electron Paramagnetic Resonance, Oxford University Press: New York, p. 291 (1990).

35. J.A. Weil, J.R. Bolton and J.E. Wertz, Electron Paramagnetic Resonance: Elementary Theory and Practical Applications, A Wiley-Interscience Publication, p. 142 (1994).

36. C.J. Ballhausen and H.B. Gray, *Inorg. Chem.*, **1**, 111 (1962);
    https://doi.org/10.1021/ic50001a022.

37. D.N. Sathyanarayana, Electronic Absorption Spectroscopy and Related Techniques, Universities Press, p. 243 (2001).

38. R. Muncaster and S. Parke, *J. Non-Cryst. Solids*, **24**, 399 (1977);
    https://doi.org/10.1016/0022-3093(77)90107-7.

39. A. Murali, J.L. Rao and A.V. Subbaiah, *J. Alloys Compd.*, **257**, 96 (1997);
    https://doi.org/10.1016/S0925-8388(96)03122-2.